Draft version January 13, 2017
Preprint typeset using LaTeX style emulateapj v. 5/2/11

arXiv:1611.04731v2 [astro-ph.CO] 12 Jan 2017

REVISITING STUDIES OF THE STATISTICAL PROPERTY OF A STRONG GRAVITATIONAL LENS SYSTEM AND MODEL-INDEPENDENT CONSTRAINT ON THE CURVATURE OF THE UNIVERSE

Jun-Qing Xia[1,*], Hai Yu[2,3,1], Guo-Jian Wang[1], Shu-Xun Tian[1], Zheng-Xiang Li[1], Shuo Cao[1], Zong-Hong Zhu[1]
[1]Department of Astronomy, Beijing Normal University, Beijing 100875, China; xiajq@bnu.edu.cn
[2]School of Astronomy and Space Science, Nanjing University, Nanjing 210093, China and
[3]Key Laboratory of Modern Astronomy and Astrophysics (Nanjing University), Nanjing 210093, China
Draft version January 13, 2017

ABSTRACT

In this paper we use a recently compiled data set, which comprises 118 galactic-scale strong gravitational lensing (SGL) systems to constrain the statistic property of SGL system, as well as the curvature of universe without assuming any fiducial cosmological model. Based on the singular isothermal ellipsoid (SIE) model of SGL system, we obtain that the constrained curvature parameter $\Omega_{\rm k}$ is close to zero from the SGL data, which is consistent with the latest result of planck measurement. More interestingly, we find that the parameter f in the SIE model is strongly correlated with the curvature $\Omega_{\rm k}$. Neglecting this correlation in the analysis will significantly overestimate the constraining power of SGL data on the curvature. Furthermore, the obtained constraint on f is different from previous results: $f = 1.105 \pm 0.030$ (68% C.L.), which means that the standard singular isothermal sphere (SIS) model ($f = 1$) is disfavored by the current SGL data at more than 3σ confidence level. We also divide the whole SGL data into two parts according to the centric stellar velocity dispersion $\sigma_{\rm c}$ and find that the larger value of $\sigma_{\rm c}$ the subsample has, the more favored the standard SIS model is. Finally, we extend the SIE model by assuming the power-law density profiles for the total mass density, $\rho = \rho_0(r/r_0)^{-\alpha}$, and luminosity density, $\nu = \nu_0(r/r_0)^{-\delta}$, and obtain the constraints on the power-law indexes: $\alpha = 1.95 \pm 0.04$ and $\delta = 2.40 \pm 0.13$ at 68% confidence level. When assuming the power-law index $\alpha = \delta = \gamma$, this scenario is totally disfavored by the current SGL data, $\chi^2_{\rm min,\gamma} - \chi^2_{\rm min,SIE} \simeq 53$.

Subject headings: gravitational lensing: strong – cosmological parameters – cosmology: theory

1. INTRODUCTION

The curvature of universe, which is often parameterized by $\Omega_{\rm k}$, is a fundamental parameter in cosmology. It determines whether our universe is open ($\Omega_{\rm k} > 0$), flat ($\Omega_{\rm k} = 0$) or close ($\Omega_{\rm k} < 0$). Currently, most of cosmological observations favor that $\Omega_{\rm k}$ is very close to zero, such as the latest constraint from the Planck measurement, $|\Omega_K| < 0.005$ (Planck Collaboration et al. 2015). However, these constrains on $\Omega_{\rm k}$ are obtained by using a model-dependent method. Therefore, constraints on curvature using the model-independent method is still very attractive in the literature (Bernstein 2006; Clarkson et al. 2007; Oguri et al. 2012; Li et al. 2014; Räsänen et al. 2015; Cai et al. 2016; Yu & Wang 2016). For instance, in Bernstein (2006), based on the basic distance sum rule, they used the weak lensing to test the curvature in a model-independent way. Recently, this method was also used in Räsänen et al. (2015) with the strong gravitational lensing (SGL) systems to test the curvature of universe and the Friedmann-Lemaître-Robertson-Walker (FLRW) metric. Räsänen et al. (2015) collected 38 SGL systems and used them to constrain $\Omega_{\rm k}$ and found that the SGL sample gives the consistent constraint with the flat universe although the statistical error is very large, $-1.22 < \Omega_{\rm k} < 0.63$ at 95% confidence level.

As an important prediction of the General Relativity (GR), SGL has become a powerful tool to test cosmology, astrophysics (the structure, formation, and evolution of galaxies and galaxy clusters), and the gravity theories. The first discovery of the SGL system Q0957+561 (Walsh et al. 1979) hints us the possibility of using the galactic lensing systems in the study of cosmological parameters and the galaxy structure. In a specific strong-lensing system, the background source (high-redshift quasar, supernova or galaxy) will reveal itself as multiple images, due to the gravitational field of the intervening lens (usually an elliptical galaxy) between the observer and the source. Meanwhile, as the image separation in the system depends on angular diameter distances to the lens and to the source, the observation of SGL can provide the information of a distance ratio $d_{\rm ls}/d_{\rm s}$, where $d_{\rm ls}$ is the angular diameter distance between the source and lens and $d_{\rm s}$ is that between the the source and observer. Following this direction, many recent works provided successful applications of different SGL samples in the investigation of the structure and evolution of galaxies (Zhu & Wu 1997; Treu et al. 2006; Cao et al. 2016), the post-Newtonian parameter describing the deviations from the GR (Schwab et al. 2010), the dynamical properties of dark energy (Zhu 2000; Chae et al. 2004; Cao et al. 2015; Li et al. 2016), and the curvature of our universe (Bernstein 2006; Räsänen et al. 2015).

Furthermore, precise spectroscopic and astrometric observations, obtained with well-defined selection criteria, may help us to study the statistic properties of lensing galaxies. Compared with late-type and unknown-type galaxies, early-type galaxies (or elliptical galaxies) which contains most of the stellar mass in the universe, provide most of the lensing galaxies in the available galactic SGL systems. Therefore, the singular isothermal ellipsoid (SIE) model, which has a elliptical projected mass distribution (Ratnatunga et al. 1999), and the singular

isothermal sphere (SIS) model, which has a spherical symmetrical mass distribution, are two useful assumptions and good first-order approximations in statistical gravitational lensing studies. For a SIE lens, the Einstein radius of a SGL system can be calculated by the theoretical expression that

$$\theta_{\rm E} = 4\pi\frac{f^2\sigma_{\rm c}^2}{c^2}\frac{d_{\rm ls}}{d_{\rm s}} \ , \tag{1}$$

where $\theta_{\rm E}$ is the Einstein radius, $\sigma_{\rm c}$ is the central velocity dispersion of the lensing galaxy , c is the speed of light and f is a phenomenological coefficient which includes several systematic errors caused by: the difference between the observed stellar velocity dispersion and that of the SIS model, the assumption of SIS model in calculating the theoretical Einstein radius, and the softened isothermal sphere potentials (Ofek et al. 2003; Cao et al. 2012). For the standard SIS model, the coefficient parameter reduces to $f = 1$. In order to take the uncertainty of f into account, a prevalent procedure in the literature is to directly include a prior on f^2 with the 20% uncertainty in the analysis. This method was firstly introduced by Kochanek et al. (2000); Ofek et al. (2003), and extensively applied in the recent works by Räsänen et al. (2015); Holanda et al. (2016). However, the statistical feature of the parameter f is still not well understood.

Recently, based on a gravitational lens dataset including 70 galactic systems from Sloan Lens ACS (SLACS) and Lens Structure and Dynamics survey (LSD), Cao et al. (2012) treated f as a free-parameter to fit the matter energy density $\Omega_{\rm m}$ and the equation of state of dark energy w. In the framework of a flat universe, their results showed that on the statistical level the 68% C.L. constraint is $f^2 = 1.01 \pm 0.02$. However, in a more recent work by Räsänen et al. (2015), the authors found that the parameter f might be correlated with the cosmic curvature $\Omega_{\rm k}$, although they did not fully take the uncertainty of f into account properly. Given the availability of a new sample of 118 lenses (Cao et al. 2015) observed by the Sloan Lens ACS Survey (SLACS), BOSS emission-line lens survey (BELLS), Lens Structure and Dynamics (LSD), and Strong Lensing Legacy Survey (SL2S), the purpose of this work is to reconsider the studies on the curvature from this latest SGL system and fully consider the effect of the uncertainty of the parameter f in the analysis. The structure of this paper is organized as follows. In Sec. 2 we will introduce the method and the SGL data used in this work. Then we will show our numerical result in Sec. 3. Finally, some discussion and summary will be in Sec. 4.

2. METHOD AND DATA

2.1. *Distance Sum Rule Method*

The basic distance sum rule is a simple geometric rule. Imaging that there are three points A, B and C on a straight line and B lies between A and C, the distances among them are $d_{\rm AB}$, $d_{\rm AC}$ and $d_{\rm BC}$, respectively. Then, obviously, there is a relation that $d_{\rm AC} = d_{\rm AB} + d_{\rm BC}$. However, if this line is not straight, the relation will become invalid. For example, assuming the line is a part of arc, then we have $d_{\rm AC} < d_{\rm AB} + d_{\rm BC}$. This rule is the same in the universe. Considering a SGL system in the universe, the distances between the observer and the lens galaxy and the sources are $d_{\rm l}$ and $d_{\rm s}$, respectively, while the distance between the lens galaxy and the source is $d_{\rm ls}$. Therefore, we have the equation $d_{\rm s} = d_{\rm l} + d_{\rm ls}$ if our universe is flat ($\Omega_{\rm k} = 0$). Otherwise, there is $d_{\rm s} > d_{\rm l} + d_{\rm ls}$ or $d_{\rm s} < d_{\rm l} + d_{\rm ls}$ for $\Omega_{\rm k} < 0$ or $\Omega_{\rm k} > 0$, respectively (see figure 1 of Bernstein (2006) for an illustration).

In the FLRW metric, the dimensionless comoving angular diameter distance between the lens galaxy, $z_{\rm l}$, and the source, $z_{\rm s}$, on a certain direction can be expressed as

$$\begin{aligned} d(z_{\rm l}, z_{\rm s}) &= (1+z_{\rm s})H_0 D_{\rm A}(z_{\rm l}, z_{\rm s}) \\ &= \frac{1}{\sqrt{|\Omega_{\rm k}|}}{\rm sinn}\left[\sqrt{|\Omega_{\rm k}|}\int_{z_{\rm s}}^{z_{\rm l}}\frac{dz'}{E(z')}\right] \ , \end{aligned} \tag{2}$$

where ${\rm sinn}(x\sqrt{|\Omega_{\rm k}|})/\sqrt{|\Omega_{\rm k}|} = \sin(x)$, x, $\sinh(x)$ if $\Omega_{\rm k} <$ $0, = 0, > 0$, respectively. $E(z) = H(z)/H_0$ is the reduced Hubble parameter at redshift z and H_0 is the Hubble constant. Therefore, $d_{\rm l}$, $d_{\rm s}$ and $d_{\rm ls}$ are equal to $d(z_{\rm l}) = d(0, z_{\rm l})$, $d(z_{\rm s}) = d(0, z_{\rm s})$ and $d(z_{\rm l}, z_{\rm s})$, respectively. Based on Equation (2), one can derive the ratio of $d_{\rm ls}$ and $d_{\rm s}$ as the function of $\Omega_{\rm k}$, $d_{\rm l}$ and $d_{\rm s}$ (Peebles 1993; Räsänen et al. 2015):

$$\frac{d_{\rm ls}}{d_{\rm s}} = \sqrt{1+\Omega_{\rm k}d_{\rm l}^2} - \frac{d_{\rm l}}{d_{\rm s}}\sqrt{1+\Omega_{\rm k}d_{\rm s}^2}. \tag{3}$$

Therefore, if we obtain the direct distance information of $d_{\rm l}$, $d_{\rm s}$ and $d_{\rm ls}$ from the observations, the determination of the curvature $\Omega_{\rm k}$ can be derived straightforwardly from the observational data using this equation without introducing any fiducial model.

Fortunately, we can extract the distance information of $d_{\rm ls}/d_{\rm s}$ directly from the observation of the SGL system through the Equation (1):

$$\frac{d_{\rm ls}}{d_{\rm s}} = \frac{\theta_{\rm E}c^2}{4\pi f^2\sigma_{\rm c}^2} \ . \tag{4}$$

In this paper, we used a comprehensive compilation of 118 strong lensing systems observed by four surveys: SLACS, BELLS, LSD and SL2S, which is also the largest gravitational lens sample published in the recent work (Cao et al. 2015). The SLACS data comprise 57 strong lenses presented in Bolton et al. (2008); Auger et al. (2009), the BELLS data comprise 25 lenses taken from Brownstein et al. (2012), then 5 most reliable lenses from the LSD survey were taken from Koopmans & Treu (2003); Treu & Koopmans (2002, 2004), and the SL2S data for a total of 31 lenses were taken from Sonnenfeld et al. (2013a,b).

The Einstein radius θ_E is defined to be the radius at which the mean surface mass density Σ equals the critical density Σ_{cr} of the lensing configuration. However, for the lens galaxies one needs to assume an specific lens model to obtain the measurements of Einstein radii from observed strong lens systems in various lensing surveys. For all of the lenses from LSD, SLACS, BELLS and SL2S used in this paper, the resulted Einstein radii were obtained on the base of a singular isothermal ellipsoid (SIE) lens-mass model. Compared with the singular isothermal sphere (SIS) counterpart, SIE includes a two-dimensional potential of similar concentric and aligned elliptical iso-density contours, with minor-to-major axis ratio $q_{\rm SIE}$ (Kassiola & Kovner 1993;

Kormann et al. 1994; Keeton & Kochanek 1998). We remark here that, although the resulted Einstein radii are slightly model dependent and SIE might not be accurate enough for some cosmological applications (Saha 2000; Rusin et al. 2002), the assumption of an SIE model does not significantly bias the determination of the value of Einstein radii used in our analysis (See Sonnenfeld et al. (2013a,b) for details).

In this SGL data, they provided 118 SGL systems with detailed information about the redshift of lens and source galaxies $z_{\rm l}$ and $z_{\rm s}$, the Einstein Radius $\theta_{\rm E}$ and the central stellar velocity dispersion $\sigma_{\rm c}$. The lens galaxies of these 118 SGL systems spread in redshift range $0.075 \leq z \leq 1.004$ and the source galaxies spread in redshift range $0.196 \leq z \leq 3.595$. In practice, we subtract those SGL systems with $z_{\rm s} > 1.4$, because the maximal redshift of the supernovae dataset we are using to determinate the cosmological distance is about 1.4 (see details in the next subsection). Finally, there are 83 SGL systems (20 samples from BELLS, 57 samples from SLACS and 6 samples from SL2S) left in our sample.

2.2. *Determination the Distances*

In order to constrain the curvature of universe using the Equation (3), we still need to have the distance information of $d_{\rm l}$, $d_{\rm s}$, besides the distance ratio $d_{\rm ls}/d_{\rm s}$. To avoid the model-dependence, here we do not use the standard ΛCDM model to calculate the dimensionless comoving angular diameter distance information. Instead, we use the current observation of the type Ia supernova (SN) to determine the distance of lens galaxy $d_{\rm l}$ and the source galaxy $d_{\rm s}$. Suzuki et al. (2012) provided the SNIa Union2.1 compilation of 580 dataset from the Hubble Space Telescope Supernova Cosmology Project. The data are usually presented as tabulated distance modulus with errors. In this catalog, the redshift spans $0 < z < 1.414$, and about 95% samples are in the low redshift region $z < 1$. The authors also provided the covariance matrix of data with and without systematic errors. In order to be conservative, we include systematic errors in our calculations.

Each SN sample in the Union 2.1 compilation gives the redshift z and the luminosity distance $d_{\rm L}$. Using the relation between comoving angular diameter distance and luminosity distance, we can obtain that

$$d(z) = \frac{H_0 d_{\rm L}(z)}{c(1+z)} \ . \tag{5}$$

It should be pointed out that the parameters of SN sample in Union 2.1 compilation are fitted with the parameters of cosmological model simultaneously. Therefore, the distance information of SN data are dependent on the input cosmological model. However, this effect caused by the assumed cosmological model can be omitted compared with the current larger uncertainties in modeling the SGL systems (Räsänen et al. 2015). Therefore, we simply use the distances and the uncertainties of the Union2.1 compilation reported in Suzuki et al. (2012).

There are several methods to use the SN data to calibrate the distance, such as the Padé approximation of order $(3, 2)$ (Liu & Wei 2015; Lin et al. 2016) and the linear or cubic interpolation method (Liang et al. 2008; Wang et al. 2016). In this work, we use a simple third-order polynomial function with constraint conditions that $d(0) = 0$ and $d'(0) = 1$ to fit the distance information of SN. It can be expressed as

$$d(z) = z + a_1 z^2 + a_2 z^3 \ , \tag{6}$$

where $a_{\rm i}$ are two free parameters which can be constrained from the SN Union2.1 compilation. Consequently, we can get the distance information of $d_{\rm l}$ and $d_{\rm s}$ from the SN observational data. Going from the third-order case to the fourth-order case does not improve the goodness of fit, which indicates that the third-order polynomial function is sufficient.

3. RESULT

In our analysis, we perform a global fitting using the COSMOMC package (Lewis & Bridle 2003), a Monte Carlo Markov chain (MCMC) code. In the program, we make several modifications which allow us using the SGL data to constrain the curvature of universe. In the calculations, we have some free parameters which should be constrained from the SGL and SN datasets simultaneously:

$$\mathbf{P} = (a_1, a_2, \Omega_{\rm k}, {\rm SGL_i}) \ , \tag{7}$$

where $\rm SGL_i$ denote the free parameter of the specific model of the SGL system. Furthermore, in the FLRW framework, if the curvature $\Omega_{\rm k} < 0$ the space will be a hypersphere and the comoving angular diameter distance will have an upper limit $d(z) \leq 1/\sqrt{-\Omega_{\rm k}}$. The current observation of cosmic microwave background radiation (CMBR) gives the angular diameter distance at $z = 1090$ is about $D_{\rm A}(1090) = 12.8 \pm 0.07\,{\rm Mpc}$ (Vonlanthen et al. 2010; Audren et al. 2013; Audren 2014). In the meanwhile we also have the direct probe on the current Hubble constant H_0 obtained from the re-analysis of Riess et al. (2011) Cepheid data made by Efstathiou (2014) by using a revised geometric maser distance to NGC 4258 from Humphreys et al. (2013): $H_0 = 72.5 \pm 2.5\,{\rm km/s/Mpc}$. Therefore, we add a prior about the lower limit of the curvature:

$$\Omega_{\rm k} \geq -\frac{c}{D_{\rm A}(1090)(1+1090)H_0} \simeq -0.1 \ . \tag{8}$$

3.1. *SIE Model*

We start from the SIE model of the SGL system. In this model, we only need one free parameter f to describe the SGL system using Equation (4).

Firstly, we try to reproduce the numerical results of model Ia in Räsänen et al. (2015) which were obtained from a small sample of SGL system. Following their steps, we take $f = 1$ and assign an error of 2% on $\theta_{\rm E}$ and a minimum error of 5% on $\sigma_{\rm c}$. In figure 1, the black solid line in the one-dimensional distribution plot of $\Omega_{\rm k}$ is the result we obtain. The 95% C.L. upper limit of the curvature: $\Omega_{\rm k} < 0.84$, which is similar with the result in the previous work (Räsänen et al. 2015).

Then, we take the uncertainty of f into account in the analysis. Different from the method in Räsänen et al. (2015), in which they assigned an extra Gaussian error of 20% on $d_{\rm ls}/d_{\rm s}$ from f^2, we treat the parameter f as a free parameter and obtain the constraints on both f and the curvature Ω_k from the SGL data simultaneously.

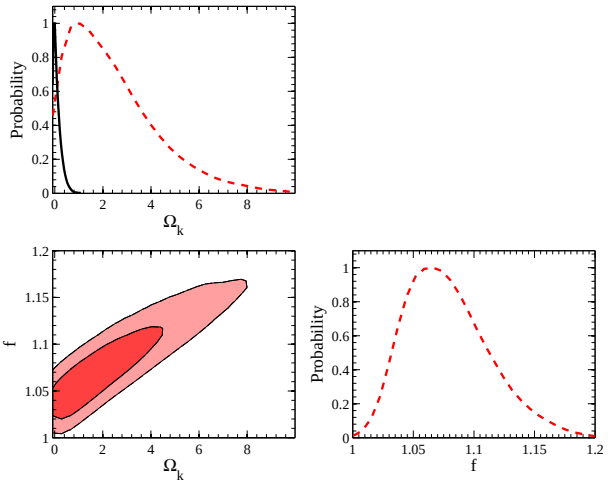

FIG. 1.— The 1-D and 2-D marginalized distributions with 1σ and 2σ contours for the parameters Ω_k and f constrained from the 23 SGL samples which were used for model Ia in Räsänen et al. (2015). For comparison, we also show the one-dimensional distribution of Ω_k by fixing $f = 1$ (black solid line).

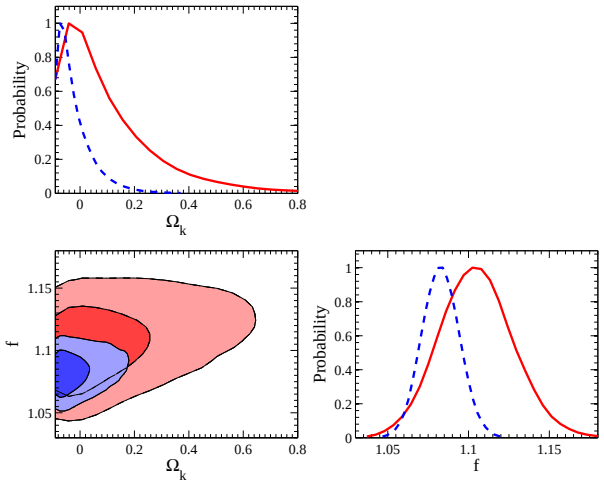

FIG. 2.— The 1-D and 2-D marginalized distributions with 1σ and 2σ contours for the parameters Ω_k and f constrained from the 83 SGL samples with (red) and without (blue) including the intrinsic scatter $\sigma_{\rm int}$ in the analysis.

The obtained one-dimensional and two-dimensional constraints on Ω_k and f are plotted in Figure 1. We find that the constraint on the curvature is quite different from the result presented in Räsänen et al. (2015). The 95% upper limit of the curvature is:

$$\Omega_k < 7.02 \ , \tag{9}$$

which is much weaker than that obtained in the case with $f = 1$. The reason is that the curvature is strongly correlated with the parameter f of the SGL system, as shown in the left-bottom panel of Figure 1. And the SGL data do not favor the standard SIS model at more than 2σ confidence level:

$$f = 1.079 \pm 0.034 \ \ (68\%\ \text{C.L.}) \ . \tag{10}$$

If we force to set the parameter $f = 1$, the obtained constraint on Ω_k will be obviously biased. The constraining power of the SGL data is significantly overestimated. Furthermore, we also notice that our result is much weaker than that obtained for model Ib in Räsänen et al. (2015) which included an extra Gaussian error of 20% on $d_{\rm ls}/d_{\rm s}$ from f^2. The reason is that including an extra Gaussian error from f^2 does not fully take the effect of f into account. The strong correlation we find here is totally neglected in the analysis. Since this strong degeneracy between f and Ω_k is broken in their analysis, the constraint on Ω_k becomes significantly tight. Furthermore, the current SGL data can already give very good constraint on f, see equation (10), the uncertainty of f^2 is much smaller than 20%.

Now we use the latest observation with 83 SGL samples to perform the global analysis. In Figure 2 we show the one-dimensional and two-dimensional constraints on Ω_k and f from the SGL data (blue dashed lines). Apparently, this new SGL data provide much stronger constraining power on Ω_k and f than the above small SGL sample used in Räsänen et al. (2015), since the strong degeneracy between Ω_k and f is partly broken. Consequently, the constraints on Ω_k and f are much tighter than above:

$$\begin{aligned} &\Omega_k < 0.16 \ \ (95\%\ \text{C.L.}) \ , \\ &f = 1.083 \pm 0.011 \ \ (68\%\ \text{C.L.}) \ . \end{aligned} \tag{11}$$

We also check the minimal χ^2 value of the best-fit model and find that $\chi^2_{\rm min} = \chi^2_{\rm SN} + \chi^2_{\rm SGL} = 545 + 243 = 788$. The χ^2 of SN data looks normal, $\chi^2_{\rm SN}/{\rm d.o.f.} = 545/580 = 0.94$, while the SGL data give too large χ^2 value, $\chi^2_{\rm SGL}/{\rm d.o.f.} = 243/83 = 2.93$. This might imply that there are some unknown uncertainties on the SGL samples.

In order to take this unknown effect into account in the analysis, we use the D'Agostini's likelihood (D'Agostini 2005):

$$\begin{aligned} \mathcal{L}_D(\Omega_k, f, \sigma_{\rm int}) \propto &\prod_i \frac{1}{\sqrt{\sigma^2_{\rm int} + [\Delta(\sigma_{\rm c,i})]^2}} \\ &\times \exp\left[-\frac{[\sigma_{\rm c,i}({\rm th}) - \sigma_{\rm c,i}({\rm obs})]^2}{2(\sigma^2_{\rm int} + [\Delta(\sigma_{\rm c,i})]^2)}\right] \ , \end{aligned} \tag{12}$$

where $\sigma_{\rm int}$ is the intrinsic scatter which represents any other unknown uncertainties except for the observational statistical ones, $\sigma_{\rm c}({\rm th})$ and $\sigma_{\rm c}({\rm obs})$ are the theoretical prediction and observation of the central stellar velocity dispersion, and $\Delta(\sigma_{\rm c})$ is the observed statistical error bar of SGL samples. By maximizing the D'Agostini's likelihood, or, equivalently, by minimizing the χ^2, we could obtained the best-fit intrinsic scatter $\sigma_{\rm int}$ and its uncertainty. Then, we put a top-hat prior on $\sigma_{\rm int}$ and use the equation

$$\chi^2 = \sum_{\rm i=1}^{83} \frac{[\sigma_{\rm c,i}({\rm th}) - \sigma_{\rm c,i}({\rm obs})]^2}{(\sigma^2_{\rm int} + [\Delta(\sigma_{\rm c,i})]^2)} \ , \tag{13}$$

to perform the whole calculations.

In Figure 2 we also show the one-dimensional and two-dimensional constraints on Ω_k and f from the SGL data with the intrinsic scatter $\sigma_{\rm int}$ included (red solid lines).

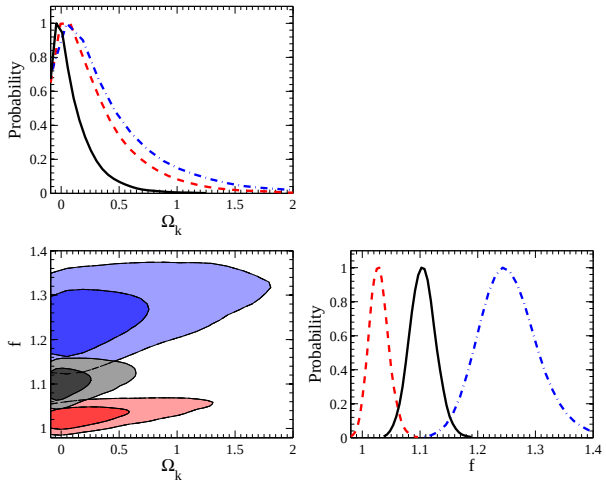

FIG. 3.— The 1-D and 2-D marginalized distributions with 1σ and 2σ contours for the parameters Ω_k and f constrained from the two subsamples with $\sigma_c < 240\,\mathrm{km/s}$ (blue dash-dotted lines) and $\sigma_c > 240\,\mathrm{km/s}$ (red dashed lines), respectively. For comparison, we also show the constraints from the whole 83 SGL samples (black solid lines).

Apparently, because the presence of the intrinsic scatter, the constraints on Ω_k and f become weaker, namely

$$\begin{aligned} \Omega_k &< 0.60 \quad (95\%\ \mathrm{C.L.})\ , \\ f &= 1.105 \pm 0.030 \quad (68\%\ \mathrm{C.L.})\ , \\ \sigma_{\rm int} &= 31.8 \pm 4.2 \quad (68\%\ \mathrm{C.L.})\ . \end{aligned} \tag{14}$$

When comparing with the CMB and baryon acoustic oscillation measurements, the constraint on the curvature from the SGL data is very weak. However, this is a model-independent constraint based only on geometrical optics, thus could be the useful complementary to model specific analyses. On the other hand, similar with above analysis, the standard SIS model with $f = 1$ is strongly disfavored by the SGL data at more than 3σ confidence level. More importantly, the minimal $\chi^2_{\rm SGL}$ now is about 85, and we obtain the reduced value $\chi^2_{\rm SGL}/\mathrm{d.o.f.} = 1.03$ consequently. Therefore, in the following calculations, we always include the intrinsic scatter $\sigma_{\rm int}$ to represent any other unknown uncertainties of the SGL data.

In order to understand the interesting constraint on the parameter f better, we first use the SGL systems in each survey to constrain f separately. As we said before, in this SGL subsample, there are 20 samples from BELLS, 57 samples from SLACS and 6 samples from SL2S. Therefore, we use 20 samples from BELLS and 57 samples from SLACS to constrain f and obtain the 68% C.L. constraints, respectively:

$$\begin{aligned} f_{\rm BELLS} &= 2.06 \pm 0.37\ , \\ f_{\rm SLACS} &= 1.07 \pm 0.03\ , \end{aligned} \tag{15}$$

which imply that the standard SIS model ($f = 1$) is still ruled out at more than 2σ confidence level in each survey. Interestingly, we find that the median value of f from BELLS is far away from the unity. However, due to the lack of SGL sample, the error bar of f from the BELLS data is very large. In meanwhile, the constraint on f from SLACS is more similar with that from all data [eq. (14)]. The constraining power on f mainly comes from the samples of SLACS survey.

Then, we divide this SGL data into two parts according the centric stellar velocity dispersion σ_c of SGL system: $\sigma_c < 240\,\mathrm{km/s}$ ($n = 41$ lenses) and $\sigma_c > 240\,\mathrm{km/s}$ ($n = 42$ lenses). In Figure 3 we show the 1-D and 2-D marginalized distributions with 1σ and 2σ contours for the parameters Ω_k and f constrained from these two subsamples. Firstly, we can see clearly, due to the smaller SGL data in two subsamples, the upper limit constraints on the curvature are weaker: $\Omega_k < 1.69$ and $\Omega_k < 1.22$ at 95% confidence level, from the small velocity dispersion subsample and large velocity dispersion subsample, respectively. Secondly, we find that the obtained constraints on the parameter f are quite different from these two subsamples. The small velocity dispersion subsample favors a large value of f:

$$f = 1.25 \pm 0.05 \quad (68\%\ \mathrm{C.L.})\ , \tag{16}$$

which means the standard SIS model with $f = 1$ is still ruled out by the data at high significance. By contrary, the large velocity dispersion subsample gives the different constraint on the parameter f:

$$f = 1.03 \pm 0.02 \quad (68\%\ \mathrm{C.L.})\ . \tag{17}$$

The standard SIS model is consistent with this large velocity dispersion subsample within 95% confidence level. The larger value of velocity dispersion σ_c the subsample has, the more favored the standard SIS model with $f = 1$ is.

Finally, we also separate this SGL data into two parts according the redshift of the lens galaxy: $z_l < 0.24$ ($n = 39$ lenses) and $z_l > 0.24$ ($n = 44$ lenses). Different from the above analysis, here we find that the constraints on f are consistent with each other at about 1σ confidence level, namely:

$$\begin{aligned} f_{z_l<0.24} &= 1.10 \pm 0.04 \quad (68\%\ \mathrm{C.L.})\ , \\ f_{z_l>0.24} &= 1.17 \pm 0.06 \quad (68\%\ \mathrm{C.L.})\ . \end{aligned} \tag{18}$$

The standard SIS model ($f = 1$) is still ruled out at more than 2σ confidence level in each subsample.

3.2. *Extended SIE Model*

Besides the standard SIE model with one free parameter f, in our analysis we also consider the more complex SGL model. As we know, the measurement of central velocity dispersion σ_c can provide a model-dependent dynamical estimate of the mass, based on the assumption of the power-law mass density profile $\rho(r)$ and luminosity density of stars $\nu(r)$:

$$\rho(r) = \rho_0 \left(\frac{r}{r_0}\right)^{-\alpha}\ , \tag{19}$$

$$\nu(r) = \nu_0 \left(\frac{r}{r_0}\right)^{-\delta}\ , \tag{20}$$

where r is the spherical radial coordinate from the lens center. Therefore, besides the parameters a_1, a_2, Ω_k and $\sigma_{\rm int}$, we have two more free parameters, α and δ. Following Cao et al. (2016), we can obtain the expression of

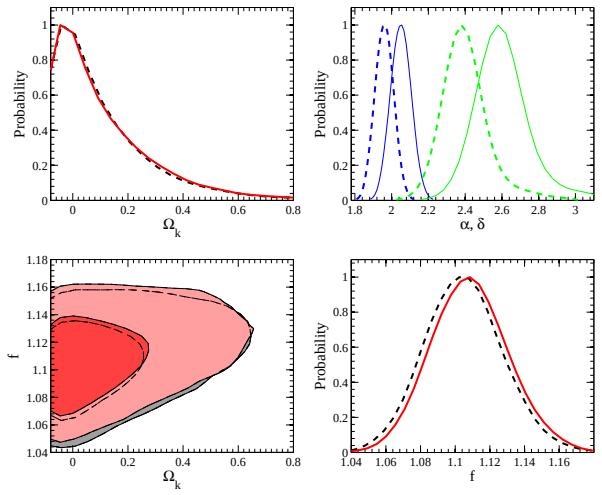

FIG. 4.— The 1-D and 2-D marginalized distributions with 1σ and 2σ contours for the parameters Ω_k and f, as well as the power-law indexes α (blue) and δ (green) with (thin solid lines) and without (thick dashed lines) considering the seeing effect, constrained from the whole 83 SGL samples. For comparison, we also show the constraints on Ω_k and f by using the simple SIE model (black lines).

the observed velocity dispersion:

$$\sigma_c^2 = \left(\frac{c^2}{4}\frac{d_s}{d_{ls}}\theta_E\right)\frac{2}{\sqrt{\pi}(\xi-2\beta)}\left(\frac{\theta_{ap}}{\theta_E}\right)^{2-\alpha} \times\left[\frac{\lambda(\xi)-\beta\lambda(\xi+2)}{\lambda(\alpha)\lambda(\delta)}\right]\frac{\Gamma\left(\frac{3-\xi}{2}\right)}{\Gamma\left(\frac{3-\delta}{2}\right)}\ , \quad (21)$$

where β is an anisotropy parameter to characterize the anisotropic distribution of three-dimensional velocity dispersion and has a Gaussian distribution $\beta = 0.18 \pm 0.13$, based on the well-studied sample of nearby elliptical galaxies from Gerhard et al. (2001), θ_{ap} is the spectrometer aperture radius, ξ has the notation $\xi = \alpha + \delta - 2$, and $\lambda(x) = \Gamma(\frac{x-1}{2})/\Gamma(\frac{x}{2})$ denotes the ratio of Euler's gamma functions. Finally, we have the χ^2 equation in the calculations

$$\chi^2 = \sum_{i=1}^{83}\left(\frac{\sigma_{c,i}(z_{l,i}, z_{s,i}, \theta_{E,i}, \theta_{ap,i}; \alpha, \delta, \beta, \sigma_{int}) - \sigma_{c,i}(obs)}{\Delta\sigma_{c,i}}\right)^2 . \quad (22)$$

In Figure 4 we show the 1-D and 2-D marginalized distributions with 1σ and 2σ contours for the parameters Ω_k and the power-law indexes α and δ constrained from the SGL data. The constraint on the curvature is identical with that obtained in the standard SIE model: $\Omega_k < 0.60$ at 95% confidence level. The power indexes α and δ can also be well-constrained, namely the 68% C.L. limits are:

$$\alpha = 1.97 \pm 0.04\ , \quad (23)$$
$$\delta = 2.40 \pm 0.13\ , \quad (24)$$

in which the constraint of α is consistent with the SIS model at 95% confidence level, while the δ constraint is ruled out the SIS model at more than 3σ confidence level. Note that, the slope δ can be directly measured from the observations, and the average mean value is $\delta = 2.39$ with 1σ error bar 0.05 (Schwab et al. 2010), which is consistent with the result we obtain here. In the calculation, the minimal χ^2 we obtain is about 84 and $\chi^2_{SGL}/d.o.f. = 1.03$, which is quite similar with those in the SIE model with the free parameter f.

We remark here that the above fitting results were obtained without considering the seeing effect. Considering the effects of aperture (θ_{ap}) with atmospheric blurring (σ_{atm}) and luminosity-weighted averaging (see Schwab et al. (2010); Cao et al. (2016) for details), the constraints become: $\alpha = 2.05 \pm 0.05$ and $\delta = 2.61 \pm 0.15$ at 68% confidence level, as shown in upper-right panel of figure 4, which is consistent with previous works (Koopmans et al. 2009; Sonnenfeld et al. 2013b; Oguri et al. 2014; Cao et al. 2016).

Furthermore, we can also derive the parameter f' by using

$$f' = \left\{\frac{2}{\sqrt{\pi}(\xi-2\beta)}\left[\frac{\lambda(\xi)-\beta\lambda(\xi+2)}{\lambda(\alpha)\lambda(\delta)}\right]\frac{\Gamma\left(\frac{3-\xi}{2}\right)}{\Gamma\left(\frac{3-\delta}{2}\right)}\right\}^{-1/2}, \quad (25)$$

and obtain the constraint from the SGL data:

$$f' = 1.108 \pm 0.030 \ \ (68\%\ \text{C.L.})\ . \quad (26)$$

Note that this term f' is different from the parameter f in the standard SIE model by a term $(\theta_{ap}/\theta_E)^{2-\alpha}$. However, this neglected term is very close to the unity when $\alpha \simeq 2$. Therefore, the posterior distribution of f' in this model and one of f in the SIE model are almost identical, see the right-bottom panel of Figure 4.

If we assume that the radial profile of the luminosity density $\nu(r)$ follows that of the total mass density $\rho(r)$, namely $\alpha = \delta = \gamma$, we can obtain the constraint:

$$\gamma = 2.04 \pm 0.02 \ \ (68\%\ \text{C.L.})\ , \quad (27)$$

which is consistent with the standard SIS model at 2σ level. And the 68% C.L. limit on the derived term is $f' = 1.00 \pm 0.01$, which is quite different from those results above. The reason is that when setting $\alpha = \delta = \gamma$, the term f' in equation (25) is limited to be not far away from the unity. As we know, the whole SGL data do not favor the model with $f = 1$. Therefore, when the term f' is close to unity by force, the minimal χ^2_{SGL} we obtain is much larger than those in the above models, $\chi^2_{min,\gamma} - \chi^2_{min,SIE} \simeq 53$. This assumption with $\alpha = \delta = \gamma$ has been ruled out by the current SGL data at very high significance.

4. DISCUSSION AND SUMMARY

Since the growing importance of SGL system in research of astronomy, investigating the statistical properties of SGL systems becomes more and more important. In this paper, we use the latest SGL data observed by four surveys: SLACS, BELLS, LSD and SL2S to study the curvature of universe model-independently, based on the basic distance sum rule method, as well as the statistical properties of SGL systems in detail. Here we summarize our main conclusions in more detail:

- Based on the standard SIS model with one free parameter f, we reproduce the analysis of

Räsänen et al. (2015) on the constraint of the curvature from a small sample of SGL data. When we fix the parameter $f = 1$, we obtain the similar constraint on the curvature with that in the previous work. However, when we set f as a free parameter, due to the strong correlation between $\Omega_{\rm k}$ and f, the constraint on the curvature is significantly enlarged, namely the 95% C.L. upper limit $\Omega_{\rm k} < 7.02$. In the meanwhile, we also obtain the limit on the parameter f: $f = 1.079 \pm 0.034$ (68% C.L.), which implies that the standard SIS model with $f = 1$ has been ruled out at more than 2σ confidence level. This result is different from that obtained in Räsänen et al. (2015), because in their analysis they did not fully take the uncertainty of f into account, but only assigned a Gaussian error of 20% from f^2. This will bring the bias on the determination of $\Omega_{\rm k}$ and overestimate the constraining power of the SGL data on the curvature.

- We perform the global analysis on the curvature and the parameter f by using the latest SGL data and find that this new SGL data can significantly improve the constraint on the curvature by a factor of 10, namely $\Omega_{\rm k} < 0.60$ (95% C.L.), when we introduce the intrinsic scatter, $\sigma_{\rm int}$, which represents any other unknown uncertainties, in the analysis. On the other hand, the constraint on the parameter f is also improved: $f = 1.105 \pm 0.030$ (68% C.L.), which tells us that the SGL data do not favor the SIS model at more than 3σ confidence level. We also use the SGL samples in each survey to constrain f separately and find that the most constraining power comes from the SLACS survey. Due to the lack of samples in BELLS survey, the limit on f is very weak.

- In order to understand this result on f better, we divide the whole SGL sample into two parts according the centric stellar velocity dispersion σ_c of SGL system: $\sigma_{\rm c} < 240\,{\rm km/s}$ and $\sigma_{\rm c} > 240\,{\rm km/s}$. Due to the smaller SGL data in two subsamples, the upper limit constraints on the curvature are weaker. More interestingly, the standard SIS model is consistent with the constraint of f from the large velocity dispersion subsample within 95% confidence level: $f = 1.03 \pm 0.02$ (2σ C.L.). The larger value of velocity dispersion $\sigma_{\rm c}$ the subsample has, the more favored the standard SIS model with $f = 1$ is. We also divide the sample into two pars according the redshift of the lens galaxy: $z_{\rm l} < 0.24$ and $z_{\rm l} > 0.24$ and find that the constraints on f are consistent with each other at about 1σ confidence level and different from the unity at more than 2σ confidence level.

- Besides the standard SIE model with one free parameter f, in our analysis we also consider the more complex SGL model by assuming the power-law mass density profile $\rho(r) = \rho_0(r/r_0)^{-\alpha}$ and luminosity density of stars $\nu(r) = \nu_0(r/r_0)^{-\delta}$. Using the whole SGL data, we obtain the constraints on the power-law indexes: $\alpha = 1.95 \pm 0.04$ and $\delta = 2.40 \pm 0.13$ at 68% confidence level, which is consistent with the direct measurement from the observations on δ. Comparing with the SIE model, we also obtain the constraint on the derived parameter f', which is almost identical with the constraint on f in the SIE model.

- We also assume that the radial profile of the luminosity density $\nu(r)$ follows that of the total mass density $\rho(r)$, namely $\alpha = \delta = \gamma$. This model strongly suggests f' is very close to the unity which is disfavored by the SGL data. Therefore, the minimal $\chi^2_{\rm SGL}$ we obtain is much larger than those in the above models, $\chi^2_{\rm min,\gamma} - \chi^2_{\rm min,SIE} \simeq 53$. This assumption with $\alpha = \delta = \gamma$ has been ruled out by the current SGL data.

ACKNOWLEDGEMENTS

J.-Q. Xia is supported by the National Youth Thousand Talents Program and the National Science Foundation of China under grant No. 11422323. G.-J. Wang, S.-X. Tian and Z.-H. Zhu are supported by the the NSFC under grant No. 11373014. H. Yu is supported by the National Basic Research Program of China (973 Program, grant No. 2014CB845800). Z.-X. Li is supported by the NSFC under grant No. 11505008. Shuo Cao is supported by the NSFC under grant No. 11503001. The research is also supported by the Strategic Priority Research Program "The Emergence of Cosmological Structures" of the Chinese Academy of Sciences, Grant No.XDB09000000, and the NSFC under grant nos. 11633001 and 11690023.

REFERENCES

Audren, B., Lesgourgues, J., Benabed, K., & Prunet, S. 2013, JCAP, 2, 001
Audren, B. 2014, MNRAS, 444, 827
Auger, M. W., et al. 2009, ApJ, 105, 1099
Bernstein, G. 2006, ApJ, 637, 598
Bolton, A. S., et al. 2008, ApJ, 682, 964
Brownstein, et al. 2012, ApJ, 744, 41
Cai, R.-G., Guo, Z.-K., & Yang, T. 2016, PRD, 93, 043517
Cao, S., Pan, Y., Biesiada, M., Godlowski, W., & Zhu, Z.-H. 2012, JCAP, 3, 016
Cao, S., Biesiada, M., Gavazzi, R., Piórkowska, A., & Zhu, Z.-H. 2015, ApJ, 806, 185
Cao, S., Biesiada, M., Yao, M., & Zhu, Z.-H. 2016, MNRAS, 461, 2192
Chae, K.-H., Chen, G., Ratra, B., & Lee, D.-W. 2004, ApJL, 607, L71
Clarkson, C., Cortês, M., & Bassett, B. 2007, JCAP, 8, 011
D'Agostini G. 2005, arXiv:physics/0511182
Efstathiou, G. 2014, MNRAS, 440, 1138
Gerhard, O., Kronawitter, A., Saglia, R. P., & Bender, R. 2001, AJ, 121, 1936
Holanda, R. F. L., Busti, V. C., & Alcaniz, J. S. 2016, JCAP, 2, 054
Humphreys, E.M.L., Reid, M.J., Moran, J.M., Greenhill, L.J., & Argon, A.L. 2013, ApJ, 775, 13
Kassiola, A., & Kovner, I. 1993, ApJ, 417, 450
Keeton, C. R., & Kochanek, C. S. 1998, ApJ, 495, 157
Kochanek, C. S., Falco, E. E., Impey, C. D., et al. 2000, ApJ, 543, 131
Koopmans, L.V.E. & Treu, T. 2003, ApJ, 583, 606
Koopmans, L.V.E. et al. 2009, ApJL, 703, L51
Kormann, R., Schneider, P., & Bartelmann, M. 1994, A&A, 284, 285
Lewis, A. & Bridle, S. 2002, PRD, 66, 103511
Li, Y.-L., Li, S.-Y., Zhang, T.-J., & Li, T.-P. 2014, ApJL, 789, L15

Li, X.-L., Cao, S., Zheng, X.-G., Li, S., & Biesiada, M. 2016, Research in Astronomy and Astrophysics, 16, 015
Liang, N., Xiao, W. K., Liu, Y., & Zhang, S. N. 2008, ApJ, 685, 354-360
Liao, K., Li, Z., Cao, S., et al. 2016, ApJ, 822, 74
Lin, H.-N., Li, X., & Chang, Z. 2016, MNRAS, 455, 2131
Liu, J., & Wei, H. 2015, General Relativity and Gravitation, 47, 141
Ofek, E. O., Rix, H.-W., & Maoz, D. 2003, MNRAS, 343, 639
Oguri, M. et al. 2012, AJ, 143, 120
Oguri, M., Rusu, C.E., & Falco, E.E. 2014, MNRAS, 439, 2494
Peebles, P. J. E. 1993, Principles of Physical Cosmology by P.J.E. Peebles. Princeton University Press, 1993. ISBN: 978-0-691-01933-8, P336
Planck Collaboration, Ade, P. A. R., Aghanim, N., et al. 2015, arXiv:1502.01589
Räsänen, S., Bolejko, K., & Finoguenov, A. 2015, Physical Review Letters, 115, 101301
Ratnatunga, K. U., Griffiths, R. E., & Ostrander, E. J. 1999, AJ, 117, 2010
Riess, A.G. et al. 2011, ApJ, 730, 119
Rusin, D., et al. 2002, MNRAS, 330, 205
Saha, P. 2000, AJ, 120, 1654
Schwab, J., Bolton, A. S., & Rappaport, S. A. 2010, ApJ, 708, 750
Sonnenfeld, A., Gavazzi, R., Suyu, S. H., Treu, T., & Marshall, P. J. 2013a, ApJ, 777, 97
Sonnenfeld, A., Treu, T., Gavazzi, R., Suyu, S. H., Marshall, P. J., Auger, M. W., & Nipoti, C. 2013b, ApJ, 777, 98
Suzuki, N., Rubin, D., Lidman, C., et al. 2012, ApJ, 746, 85
Treu, T., & Koopmans, L.V.E. 2002, ApJ, 575, 87
Treu, T., & Koopmans, L.V.E. 2004, ApJ, 611, 739
Treu, T., Koopmans, L. V., Bolton, A. S., Burles, S., & Moustakas, L. A. 2006, ApJ, 640, 662
Vonlanthen, M., Räsänen, S., & Durrer, R. 2010, JCAP, 8, 023
Walsh, D., Carswell, R. F., & Weymann, R. J. 1979, Nature, 279, 381
Wang, J. S., Wang, F. Y., Cheng, K. S., & Dai, Z. G. 2016, AAP, 585, A68
Yu, H., & Wang, F. Y. 2016, arXiv:1605.02483
Zhu, Z.-H., & Wu, X.-P. 1997, AAP, 326, L9
Zhu, Z.-H. 2000, Modern Physics Letters A, 15, 1023